Journal of Sound and Vibration (1999) **226**(4), 755–767
Article No. jsvi.1999.2315, available online at http://www.idealibrary.com on IDEAL®

SEGMENTED SENSORS AND ACTUATORS FOR THICK PLATES AND SHELLS PART II: PARAMETRIC STUDY

P. C. Dumir, G. P. Dube and C. Balaji Kumar
Applied Mechanics Department, I.I.T. Delhi, New Delhi 110016, *India*

(*Received* 16 *June* 1998, *and in final form* 12 *April* 1999

A parametric study is presented here for the modal sensitivity and actuation factors and controlled damping ratio for the rectangularly segmented distributed piezoelectric sensor and actuator layers laminated on simply supported thick rectangular plates and circular cylindrical shells made of cross ply composite laminate. The analytical expressions of these entities, developed in Part I of this two-part study, based on a Flugge-type first order shear deformation theory (FSDT) and classical lamination theory (CLT), are numerically evaluated to illustrate the effect of the thickness parameter. The contribution of the membrane and bending strains to sensitivity and actuation factors is computed for plates and shells for the lowest mode and a few higher modes. It has been concluded that the classical lamination theory is inadequate for the analysis of spatial actuation and control of all modes for thick plates and shells as well as for the higher modes of thin composite plates and shells.

1. INTRODUCTION

The sensing and actuation effect of distributed piezoelectric sensors and actuators, laminated on plates and shells depends on their shape, thickness, material properties, placement, spatial shaping and spatial distribution. The previous studies [1–4] of rectangularly segment sensors and actuators, laminated on thin plates and shells, were based on classical lamination theory (CLT) neglecting shear and rotatory inertia. The effect of shear deformation and rotatory inertia is significant for composite thin plates and shells for higher modes. Even for lower modes, these effects are important for composite plates and shells with fibre-reinforced composite elastic substrate, due to the small ratio of the transverse shear modulus to the longitudinal Young's modulus. In Part I of this study [5], analytical expressions for modal membrane and bending sensitivity factors, membrane and bending actuation factors and controlled damping ratio have been developed for the case of velocity feedback using a first order shear deformation theory (FSDT), for rectangularly segmented piezoelectric sensor and actuator layers laminated on simply supported rectangular plates and circular cylindrical shell panels made of cross-ply composite laminate. The contribution of the in-plane displacement components is included. In Part II of this work, a parametric study is presented to illustrate the effect of the thickness parameter on modal sensitivity and

0022-460X/99/390755 + 13 $30.00/0

actuation factors and the controlled damping ratio by comparing the FSDT and the CLT results for a few lower order modes.

2. RESULTS FOR PLATES

Results are presented for simply supported, square composite plates with side $a = 0{\cdot}2$ m made up of 6 layered cross-ply graphite–epoxy laminate sandwiched between two PZT layers. The bottom and top piezoelectric layers act as sensor and actuator respectively. These are quarterly segmented with $h_s/h_e = h_a/h_e = \frac{1}{40}$. The analysis is carried out for symmetric $[90^\circ/0^\circ/90^\circ]s$ and antisymmetric $[90^\circ/0^\circ/90^\circ/0^\circ/90^\circ/0]$ laminates where the orientations are given with respect to the x-axis. The material properties of graphite–epoxy and PZT used are listed in Table 1. The expressions of total sensitivity and actuation factors S^t_{mn} and A^t_{mn} are listed in Part I of this work. These are non-dimensionalized as follows:

$$S^{t*}_{mn} = S^t_{mn}\eta_{33}\rho^{1/2}_{eff}a^{1/2}/Y_2 d_{32}(h/a)^{3/2}, \qquad A^{t*}_{mn} = A^t_{mn}\rho^{1/2}_{eff}a^{3/2}/Y_2 d_{32}(h/a)^{1/2}, \quad (1)$$

where Y_2, d_{32} and η_{33} are the material parameters of PZT and $\rho_{eff} = \sum \rho_i h_i/h$ with ρ_i, h_i being the density and the thickness of the ith layer. S^{t*}_{mn}, A^{t*}_{mn} and ξ^c, obtained using CLT, are listed in Table 2 for the thin plates with $h/a = \frac{1}{100}$ for four distinct modes (1, 1), (2, 2), (1, 3) and (3, 3).

The variation of the total sensitivity factor, the total actuation factor and the controlled damping ratio ξ^c with the thickness parameter h/a has been studied using CLT and FSDT for four distinct modes. For this purpose, their values are normalized with respect to the values obtained using CLT for thin plates with $h/a = \frac{1}{100}$. The normalized values of the total sensitivity factor S^{t*}_{mn}, the total actuation factor A^{t*}_{mn} and the controlled damping ratio ξ^c for the symmetric plates using CLT and FSDT are presented in Figures 1–3. The values for the FSDT are

TABLE 1

Material properties

Property	Graphite–epoxy	PZT	Units
Y_1	181·0	61·0	GPa
Y_2	10·3	61·0	GPa
g_{23}	2·87	21·1	GPa
g_{31}	7·17	21·1	GPa
g_{12}	7·17	22·6	GPa
v_{12}	0·28	0·38	
ρ	1600	7600	kg/m^3
η_{33}	—	$1{\cdot}5 \times 10^{-8}$	F/m
d_{31}	—	-171×10^{-12}	m/V
d_{32}	—	-171×10^{-12}	m/V
d_{24}	—	584×10^{-12}	m/V
d_{15}	—	584×10^{-12}	m/V

TABLE 2

S_{mn}^{t*}, A_{mn}^{t*} and ξ^c for plate with $h/a = 0{\cdot}01$ using CLT

Plate	Mode	S_{mn}^{t*}	A_{mn}^{t*}	$10^4 \xi^c/G$
Symm.	(1, 1)	−0·03931	−38·05	13·257
	(2, 2)	−0·03931	−38·05	13·257
	(1, 3)	−0·06551	−63·42	0·741
	(3, 3)	−0·03931	−38·05	0·164
Antisymm.	(1, 1)	−0·03931	−38·05	14·037
	(2, 2)	−0·03931	−38·05	14·037
	(1, 3)	−0·05793	−70·75	1·085
	(3, 3)	−0·03931	−38·05	0·173

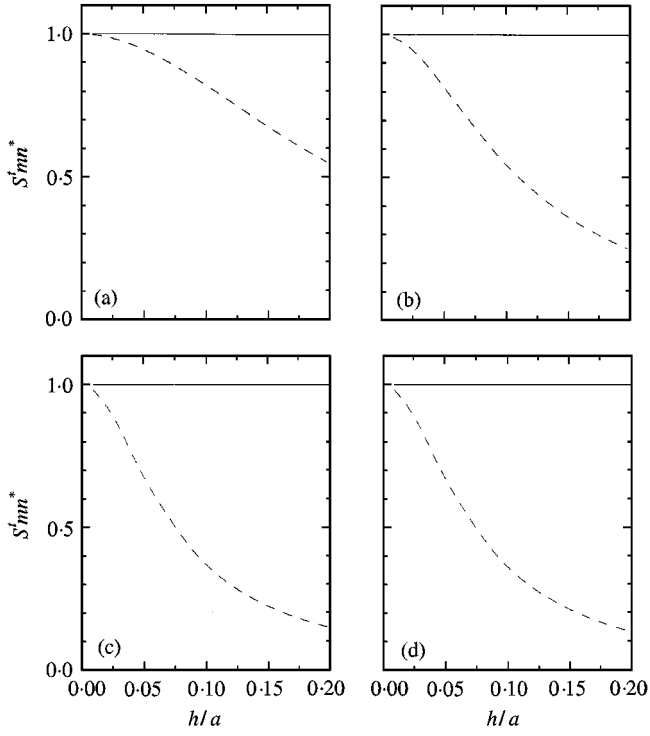

Figure 1. Effect of h/a on total sensitivity factor of symmetric plate: —— CLT; – – – FSDT; (a) $m = 1$, $n = 1$; (b) $m = 2$, $n = 2$; (c) $m = 1$, $n = 3$; (d) $m = 3$, $n = 3$.

much lower compared to the CLT for thick plates, especially for higher modes. This difference is due to the relative increase in shear deformation compared to deformation due to bending for thicker plates and higher modes. FSDT and CLT yield almost the same results for thin plates up to $h/a = \frac{1}{50}$. There is significant difference in the results for higher modes (1, 3) and (3, 3) even for $h/a = \frac{1}{20}$. The normalized sensitivity factor, actuation factor and damping ratio ξ^c of antisymmetric plates are presented in Figures 4–6. The effect of the thickness

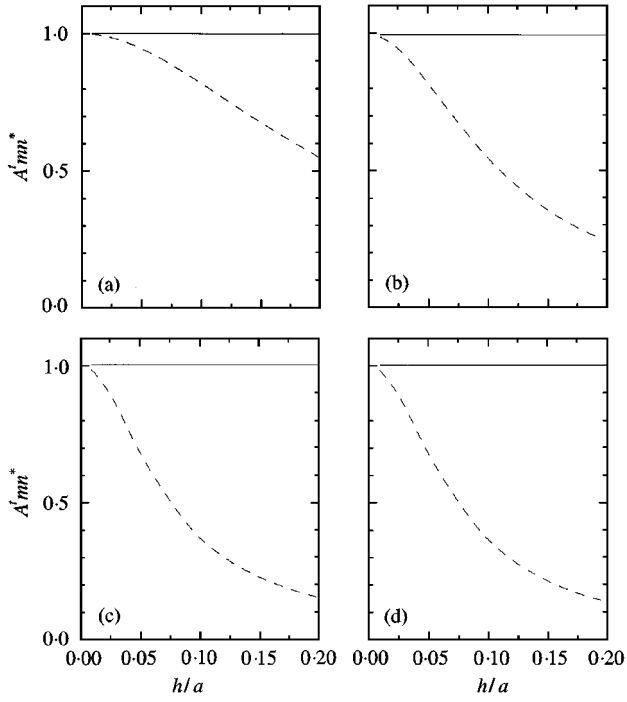

Figure 2. Effect of h/a on total actuation factor of symmetric plate: —— CLT; – – – FSDT; (a) $m = 1$, $n = 1$; (b) $m = 2$, $n = 2$; (c) $m = 1$, $n = 3$; (d) $m = 3$, $n = 3$.

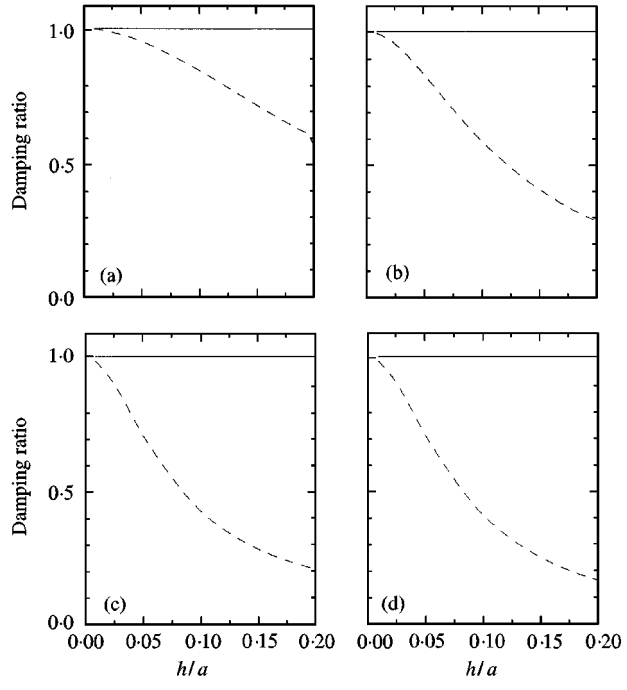

Figure 3. Effect of h/a on damping ratio of symmetric plate: —— CLT; – – – FSDT; (a) $m = 1$, $n = 1$; (b) $m = 2$, $n = 2$; (c) $m = 1$, $n = 3$; (d) $m = 3$, $n = 3$.

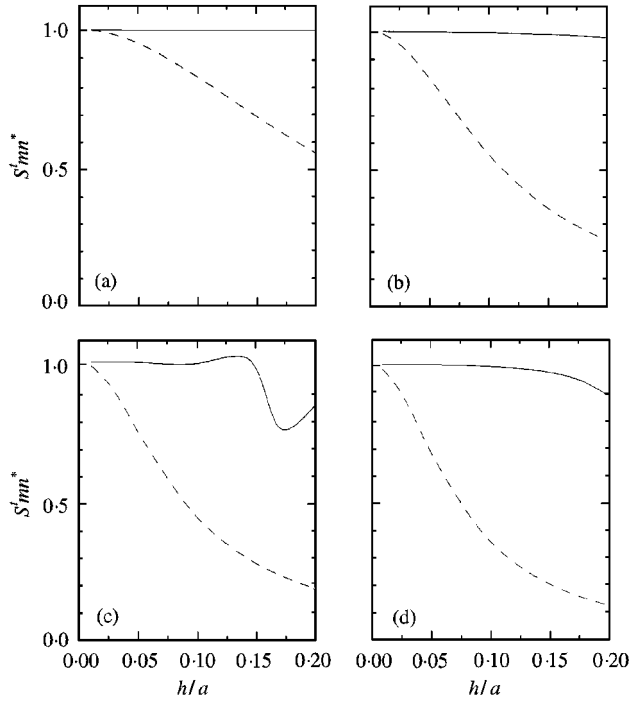

Figure 4. Effect of h/a on total sensitivity factor of antisymmetric plate: —— CLT; – – – FSDT; (a) $m = 1$, $n = 1$; (b) $m = 2$, $n = 2$; (c) $m = 1$, $n = 3$; (d) $m = 3$, $n = 3$.

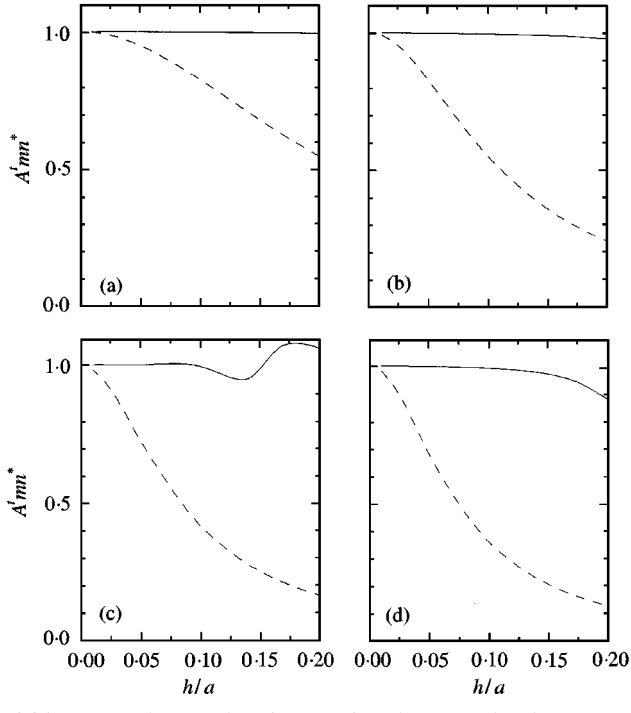

Figure 5. Effect of h/a on total actuation factor of antisymmetric plate: —— CLT; – – – FSDT; (a) $m = 1$, $n = 1$; (b) $m = 2$, $n = 2$; (c) $m = 1$, $n = 3$; (d) $m = 3$, $n = 3$.

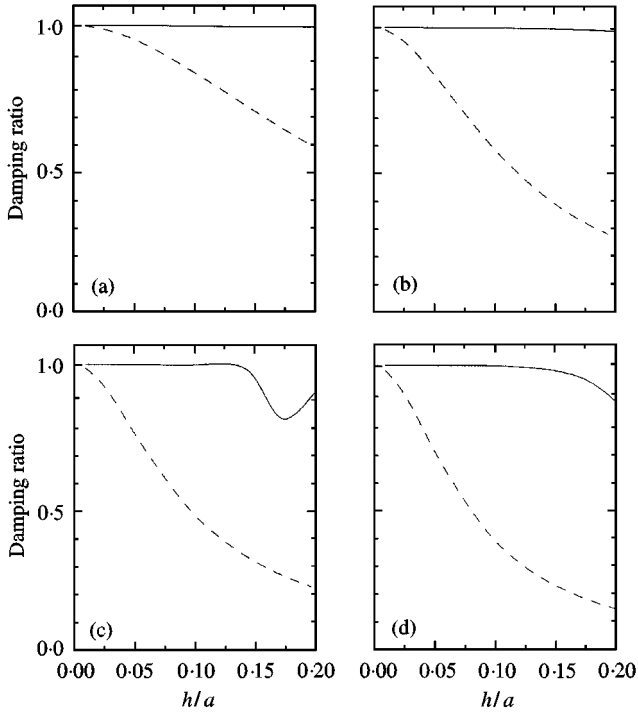

Figure 6. Effect of h/a on damping ratio of antisymmetric plate: —— CLT; – – – FSDT; (a) $m = 1$, $n = 1$; (b) $m = 2$, $n = 2$; (c) $m = 1$, $n = 3$; (d) $m = 3$, $n = 3$.

parameter h/a on S^{t*}_{mn}, A^{t*}_{mn} and ξ^c for antisymmetric plates is similar to that for the symmetric plates.

3. RESULTS FOR SHELLS

Results are presented for simply supported, circular cylindrical composite shells with $a = 0{\cdot}2$ m, $R = 0{\cdot}1$ m, $\psi = 120^\circ$, made up of six-layered cross-ply graphite–epoxy core with PZT layers at the inside and the outside. The inner and the outer piezoelectric layers act as sensor and actuator respectively. These are quarterly segmented with $h_s/h_e = h_a/h_e = \frac{1}{40}$. The analysis is carried out for symmetric $[90^\circ/0^\circ/90^\circ]_s$ and antisymmetric $[90^\circ/0^\circ/90^\circ/0^\circ/90^\circ/0^\circ]$ laminates where the orientations are given with respect to the x-axis. The expressions of bending and total sensitivity and actuation factors, S^b_{mn}, S^t_{mn} and S^s_{mn}, A^t_{mn}, listed in Part I of this work, are non-dimensionalized as follows:

$$S^{b*}_{mn} = S^b_{mn}\eta_{33}\rho^{1/2}_{eff}a^{1/2}/Y_2 d_{32}(h/R)^{3/2}, \qquad A^{b*}_{mn} = A^b_{mn}\rho^{1/2}_{eff}a^{3/2}/Y_2 d_{32}(h/R)^{1/2}, \quad (2)$$

$$S^{t*}_{mn} = S^t_{mn}\eta_{33}\rho^{1/2}_{eff}a^{1/2}/Y_2 d_{32}(h/R)^{1/2}, \qquad A^{t*}_{mn} = A^t_{mn}\rho^{1/2}_{eff}a^{3/2}(h/R)^{1/2}/Y_2 d_{32}. \quad (3)$$

S^{b*}_{mn}, S^{t*}_{mn}, A^{b*}_{mn}, A^{t*}_{mn} and ξ^c, obtained using CLT, are listed in Table 3 for thin shells with $h/R = \frac{1}{50}$ for four distinct modes (1, 1), (2, 2), (1, 3) and (3, 3).

TABLE 3

S^{b*}_{mn}, S^{t*}_{mn}, A^{b*}_{mn}, A^{t*}_{mn} and ξ^c for shell with $h/R = 0{\cdot}02$ using CLT

Shell	Mode	$10^4 S^{b*}_{mn}$	$10^4 S^{t*}_{mn}$	A^{b*}_{mn}	A^{t*}_{mn}	$10^4 \xi^c/G$
Symm.	(1, 2)	−112·2	4·525	−21·73	−1·573	−0·5977
	(2, 2)	−127·2	−0·5267	−24·63	−0·8346	0·4273
	(1, 3)	−209·9	−2·931	−40·32	−0·9828	0·5627
	(3, 3)	−130·6	−1·684	−25·29	−0·6632	0·0480
Anti-symm.	(1, 1)	−112·8	3.733	−21·84	−1·422	−0·4355
	(2, 2)	−127·6	−0·7178	−24·71	−0·8000	0·5493
	(1, 3)	−210·3	−2·653	−40·39	−1·040	0·6857
	(3, 3)	−130·9	−1·780	−25·35	−0·6468	0·0481

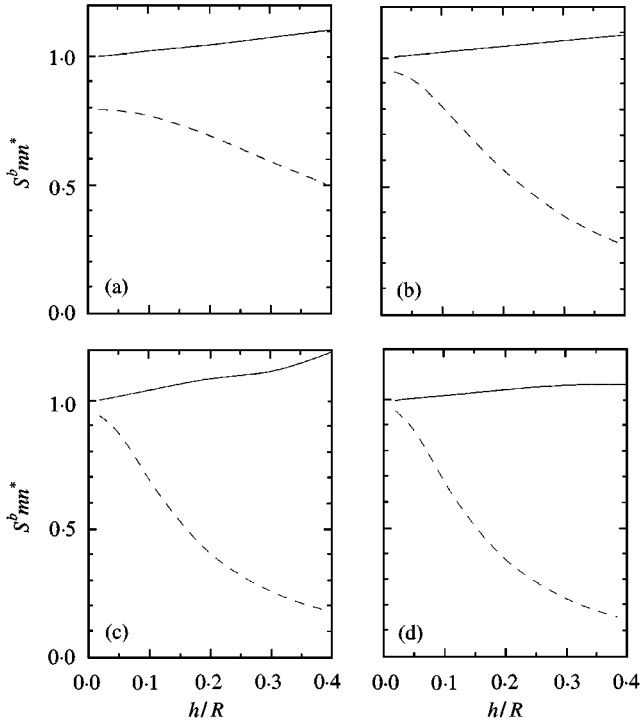

Figure 7. Effect of h/R on bending sensitivity factor of symmetric shell: —— CLT; – – – FSDT; (a) $m = 1$, $n = 1$; (b) $m = 2$, $n = 2$; (c) $m = 1$, $n = 3$; (d) $m = 3$, $n = 3$.

The variation of the bending and total sensitivity factors, the bending and total actuation factors and the controlled damping ratio ξ^c with the thickness parameter h/R have been studied using CLT and FSDT for four modes. For this purpose, their non-dimensionalized values are normalized with respect to the values obtained using CLT for thin shells with $h/R = \frac{1}{50}$. These normalized values and the controlled damping ratio ξ^c for the symmetric shells using CLT and FSDT are presented in Figures 7–11. As in the case of plates, the values for the FSDT are

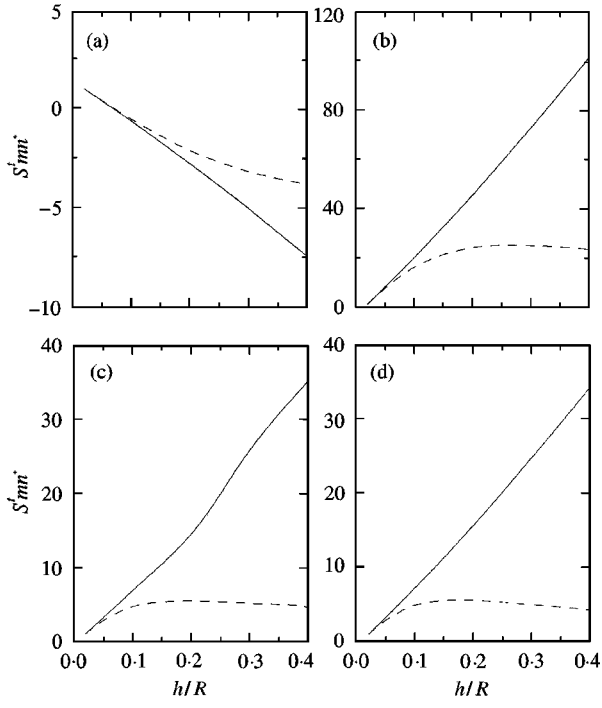

Figure 8. Effect of h/R on total sensitivity factor of symmetric shell: —— CLT; – – – FSDT; (a) $m = 1$, $n = 1$; (b) $m = 2$, $n = 2$; (c) $m = 1$, $n = 3$; (d) $m = 3$, $n = 3$.

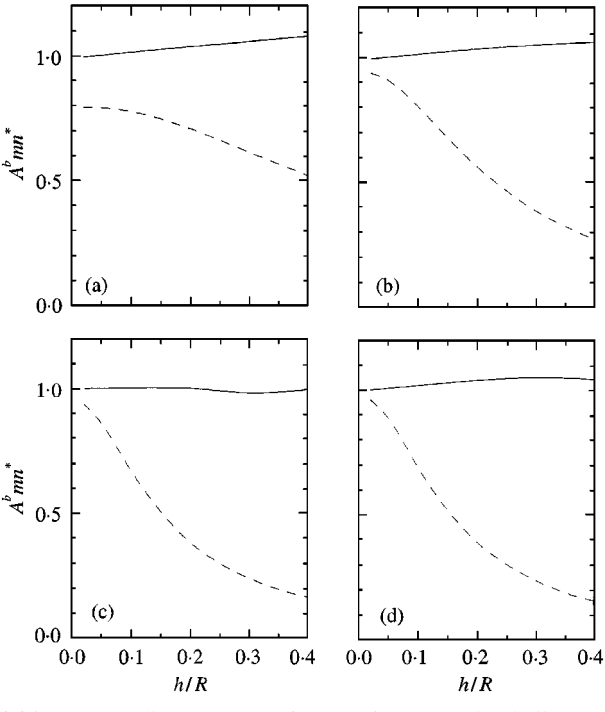

Figure 9. Effect of h/R on bending actuator factor of symmetric shell: —— CLT; – – – FSDT; (a) $m = 1$, $n = 1$; (b) $m = 2$, $n = 2$; (c) $m = 1$, $n = 3$; (d) $m = 3$, $n = 3$.

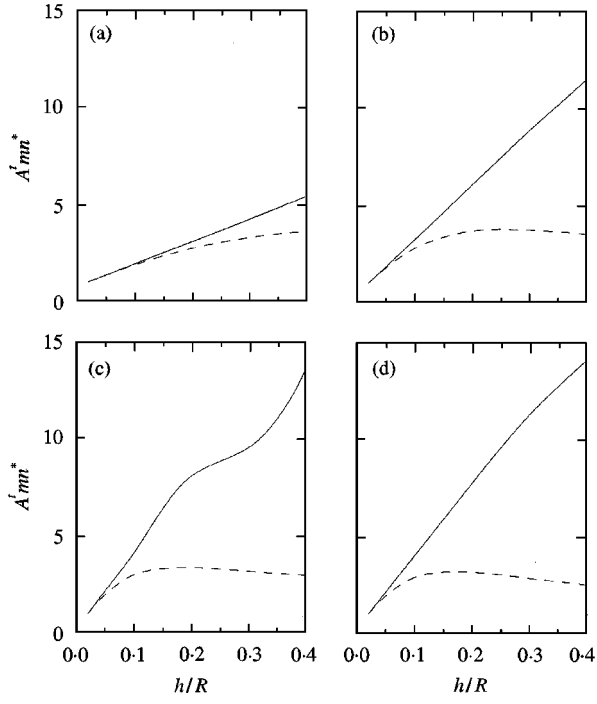

Figure 10. Effect of h/R on total actuation factor of symmetric shell: —— CLT; – – FSDT; (a) $m = 1$, $n = 1$; (b) $m = 2$, $n = 2$; (c) $m = 1$, $n = 3$; (d) $m = 3$, $n = 3$.

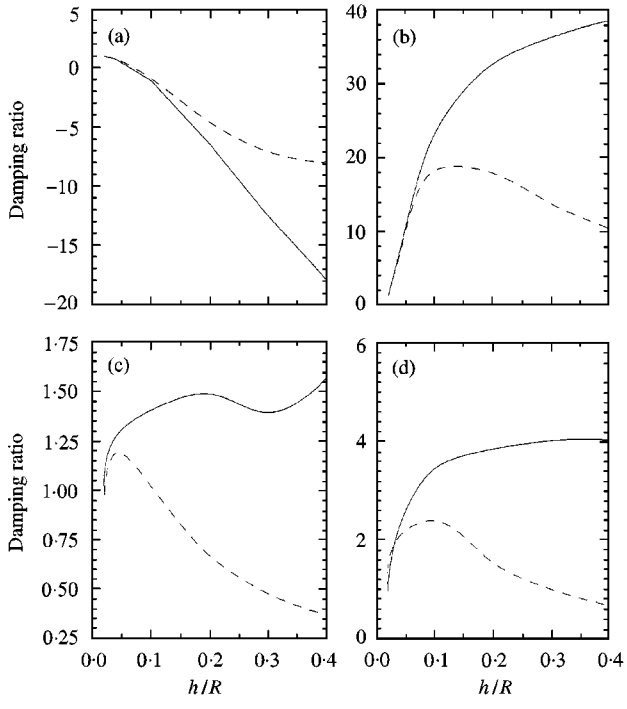

Figure 11. Effect of h/R on damping ratio of symmetric shell: —— CLT; – – – FSDT; (a) $m = 1$, $n = 1$; (b) $m = 2$, $n = 2$; (c) $m = 1$, $n = 3$; (d) $m = 3$, $n = 3$.

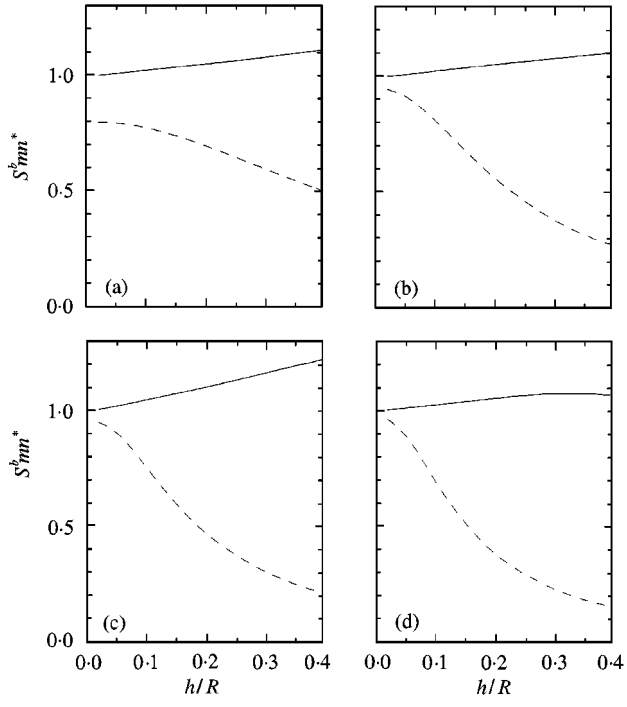

Figure 12. Effect of h/R on bending sensitivity factor of antisymmetric shell: —— CLT; – – – FSDT; (a) $m = 1$, $n = 1$; (b) $m = 2$, $n = 2$; (c) $m = 1$, $n = 3$; (d) $m = 3$, $n = 3$.

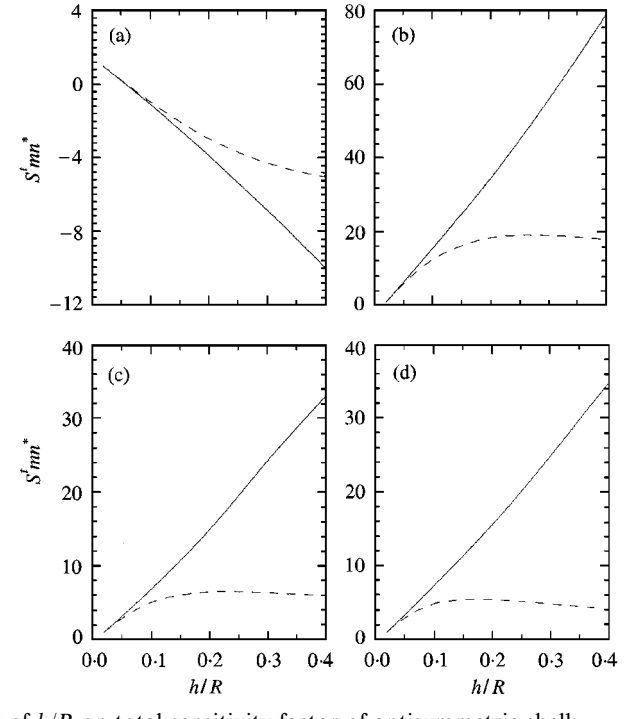

Figure 13. Effect of h/R on total sensitivity factor of antisymmetric shell: —— CLT; – – – FSDT; (a) $m = 1$, $n = 1$; (b) $m = 2$, $n = 2$; (c) $m = 1$, $n = 3$; (d) $m = 3$, $n = 3$.

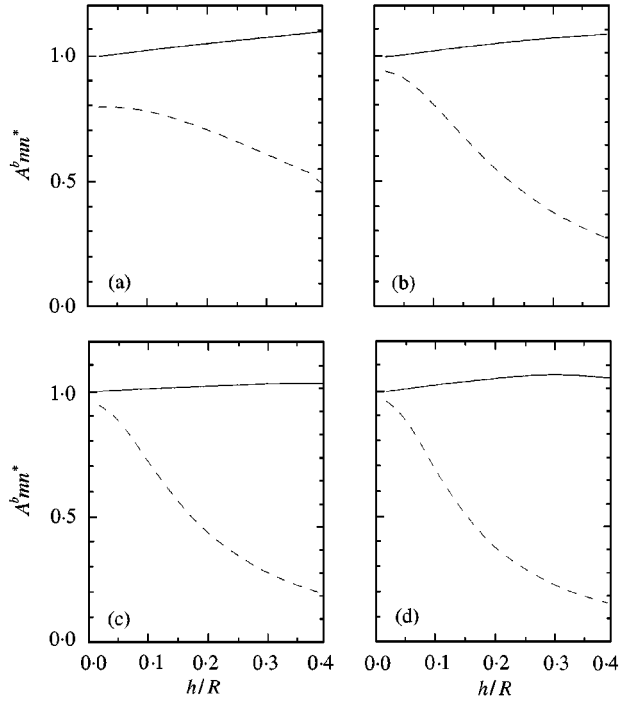

Figure 14. Effect of h/R on bending actuation factor of antisymmetric shell: —— CLT; – – – FSDT; (a) $m = 1$, $n = 1$; (b) $m = 2$, $n = 2$; (c) $m = 1$, $n = 3$; (d) $m = 3$, $n = 3$.

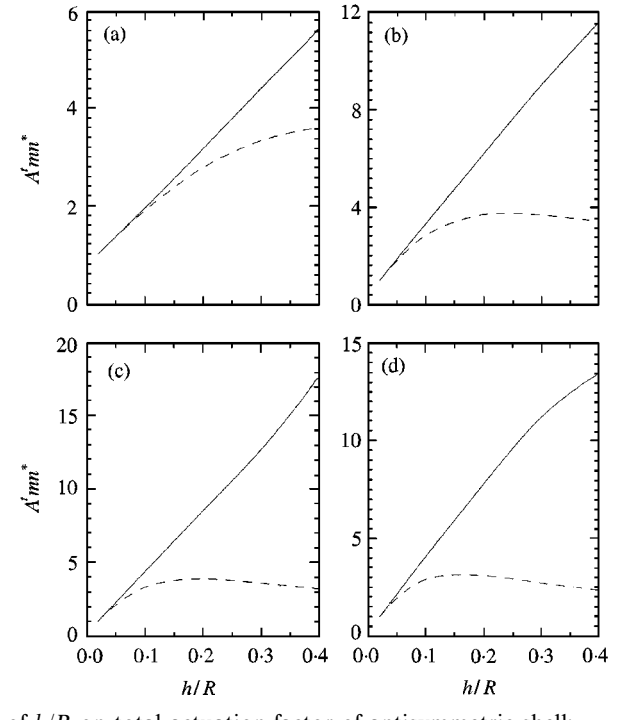

Figure 15. Effect of h/R on total actuation factor of antisymmetric shell: —— CLT; – – – FSDT; (a) $m = 1$, $n = 1$; (b) $m = 2$, $n = 2$; (c) $m = 1$, $n = 3$; (d) $m = 3$, $n = 3$.

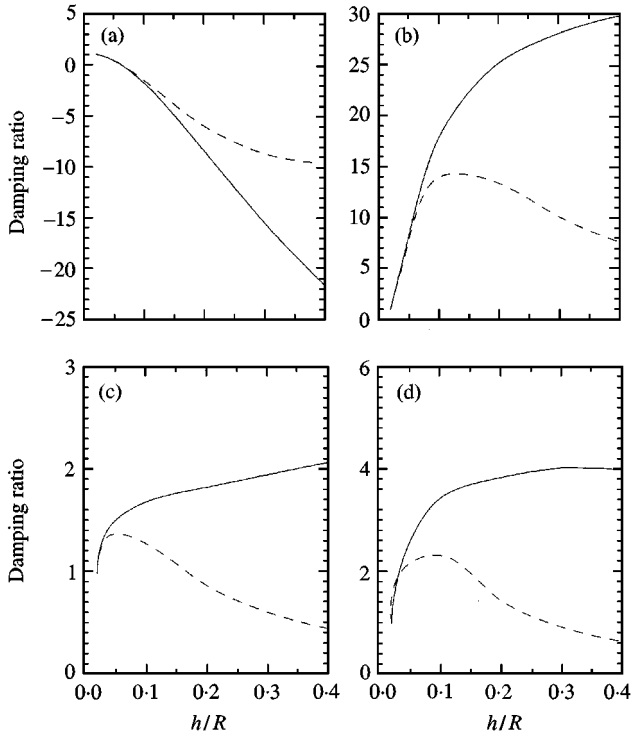

Figure 16. Effect of h/R on damping ratio of antisymmetric shell: —— CLT; – – – FSDT; (a) $m = 1$, $n = 1$; (b) $m = 2$, $n = 2$; (c) $m = 1$, $n = 3$; (d) $m = 3$, $n = 3$.

much lower compared to the CLT for thick shells, especially for higher modes since the effect of shear deformation becomes significant for thicker shells and higher modes. The normalized sensitivity factors, actuation factors and damping ratio ξ^c of antisymmetric shells are presented in Figures 12–16. The effect of thickness parameter h/R on these for antisymmetric shells is similar to that for the symmetric shells.

4. CONCLUSIONS

The theory developed in Part I of this study is applied in this work to illustrate the influence of shear deformation on the sensitivity and actuation factors of composite plates and shells with composite elastic cores. For composite-PZT plates and shells, it has been found that there is a very large discrepancy between the classical and first order shear deformation theory results, especially for higher modes. For both plates and shells, the controlled damping ratio for the higher modes is lower than that for the lower modes. Hence, a greater signal amplification factor G is needed to damp out the higher modes. In view of the large discrepancy in the results obtained using classical and first order shear deformation theories for larger thickness parameter and higher modes, it is concluded that analysis of hybrid composite plates and shells should be based on the first order shear deformation theory.

REFERENCES

1. H. S. Tzou and H. Q. Fu 1994 *Journal of Sound and Vibration* **172**, 247–259. A study of segmentation of distributed piezoelectric sensors and actuators. Part 1: theoretical analysis.
2. H. S. Tzou and H. Q. Fu 1994 *Journal of Sound and Vibration* **172**, 261–275. A study of segmentation of distributed piezoelectric sensors and actuators. Part 2: parametric study and active vibration controls.
3. H. S. Tzou, Y. Bao and V. B. Venkayya 1996 *Journal of Sound and Vibration* **197**, 207–224. Parametric study of segmented transducers laminated on cylindrical shells, Part 1: sensor patches.
4. H. S. Tzou, Y. Bao and V. B. Venkayya 1996 *Journal of Sound and Vibration* **197**, 225–249. Parametric study of segmented transducers laminated on cylindrical shells, Part 1: sensor patches.
5. G. P. Dube, P. C. Dumir and C. Balaji Kumar 1999 *Journal of Sound and Vibration* **226**, 739–753. Segmented sensors and actuators for thick plates and shells. Part I: Analysis using FSDT.